



Supplement of

Northern Hemisphere blocking simulation in current climate models: evaluating progress from the Climate Model Intercomparison Project Phase 5 to 6 and sensitivity to resolution

Reinhard Schiemann et al.

Correspondence to: Reinhard Schiemann (r.k.schiemann@reading.ac.uk)

The copyright of individual parts of the supplement might differ from the CC BY 4.0 License.

Supplement

Northern Hemisphere blocking simulation in current climate models: evaluating progress from CMIP5 to CMIP6 and sensitivity to resolution, Weather and Climate Dynamics, 2020,
5 by Reinhard Schiemann et al.

List of Figures

- 5 S7 As Fig. S3 but for the PAC domain (120-240E, 40-90N). (Metrics of blocking performance (a,b - blocking frequency, c,d - spatial correlation, e,f - root-mean-square error) for the ANOM index and boreal winter. The left-hand side of each panel shows metrics for PRIMAVERA simulations at different grid spacings (resolutions). Boxplots on the right-hand side show distributions of the metric across CMIP5 and CMIP6 simulations. The '*' symbol in the column 'ERA/IV' shows the reanalysis estimate and the boxplot is an estimate of the expected agreement given internal variability (see text.) 10 55
- 10 S8 As Fig. S3 but for the PAC domain (120-240E, 40-90N) and boreal summer. (Metrics of blocking performance (a,b - blocking frequency, c,d - spatial correlation, e,f - root-mean-square error) for the ANOM index. The left-hand side of each panel shows metrics for PRIMAVERA simulations at different grid spacings (resolutions). Boxplots on the right-hand side show distributions of the metric across CMIP5 and CMIP6 simulations. The '*' symbol in the column 'ERA/IV' shows the reanalysis estimate and the boxplot is an estimate of the expected agreement given internal variability (see text.) 11 60
- 15 S9 Persistence of blocking events (a,b - median, c,d - 90th percentile) for the ANOM index and boreal winter, for the ATL domain (-90-90E, 50-90N). The left-hand side of each panel shows metrics for PRIMAVERA simulations at different grid spacings (resolutions). Boxplots on the right-hand side show distributions of the persistence metric across CMIP5 and CMIP6 simulations. The '*' symbol in the column 'ERA/IV' shows the reanalysis estimate and the boxplot is an estimate of the expected agreement given internal variability (see text.) 12 65
- 20 S10 As Fig. S9 but for boreal summer. (Persistence of blocking events (a,b - median, c,d - 90th percentile) for the ANOM index and for the ATL domain (-90-90E, 50-90N). The left-hand side of each panel shows metrics for PRIMAVERA simulations at different grid spacings (resolutions). Boxplots on the right-hand side show distributions of the persistence metric across CMIP5 and CMIP6 simulations. The '*' symbol in the column 'ERA/IV' shows the reanalysis estimate and the boxplot is an estimate of the expected agreement given internal variability (see text.) 13 70
- 25 S11 As Fig. S9 but for the AGP index and for the PAC domain (90-270E, 50-75N). Persistence of blocking events (a,b - median, c,d - 90th percentile) for boreal winter. The left-hand side of each panel shows metrics for PRIMAVERA simulations at different grid spacings (resolutions). Boxplots on the right-hand side show distributions of the persistence metric across CMIP5 and CMIP6 simulations. The '*' symbol in the column 'ERA/IV' shows the reanalysis estimate and the boxplot is an estimate of the expected agreement given internal variability (see text.) 14 75
- 30 S12 As Fig. S9 but for the AGP index, for the PAC domain (90-270E, 50-75N), and for boreal summer. (Persistence of blocking events (a,b - median, c,d - 90th percentile). The left-hand side of each panel shows metrics for PRIMAVERA simulations at different grid spacings (resolutions). Boxplots on the right-hand side show distributions of the persistence metric across CMIP5 and CMIP6 simulations. The '*' symbol in the column 'ERA/IV' shows the reanalysis estimate and the boxplot is an estimate of the expected agreement given internal variability (see text.) 15 80
- 35 S13 As Fig. S9 but for the PAC domain (120-240E, 40-90N). (Persistence of blocking events (a,b - median, c,d - 90th percentile) for the ANOM index and boreal winter. The left-hand side of each panel shows metrics for PRIMAVERA simulations at different grid spacings (resolutions). Boxplots on the right-hand side show distributions of the persistence metric across CMIP5 and CMIP6 simulations. The '*' symbol in the column 'ERA/IV' shows the reanalysis estimate and the boxplot is an estimate of the expected agreement given internal variability (see text.) 16 85
- 40 S14 As Fig. S9 but for the PAC domain (120-240E, 40-90N) and boreal summer. (Persistence of blocking events (a,b - median, c,d - 90th percentile) for the ANOM index. The left-hand side of each panel shows metrics for PRIMAVERA simulations at different grid spacings (resolutions). Boxplots on the right-hand side show distributions of the persistence metric across CMIP5 and CMIP6 simulations. The '*' symbol in the column 'ERA/IV' shows the reanalysis estimate and the boxplot is an estimate of the expected agreement given internal variability (see text.) 17 90
- 45 S15 As Fig. S9 but for the AGP index and for the ATL domain (90-270E, 50-75N). Persistence of blocking events (a,b - median, c,d - 90th percentile) for boreal summer. The left-hand side of each panel shows metrics for PRIMAVERA simulations at different grid spacings (resolutions). Boxplots on the right-hand side show distributions of the persistence metric across CMIP5 and CMIP6 simulations. The '*' symbol in the column 'ERA/IV' shows the reanalysis estimate and the boxplot is an estimate of the expected agreement given internal variability (see text.) 18 95
- 50 S16 As Fig. S9 but for the AGP index, for the ATL domain (90-270E, 50-75N), and for boreal summer. (Persistence of blocking events (a,b - median, c,d - 90th percentile). The left-hand side of each panel shows metrics for PRIMAVERA simulations at different grid spacings (resolutions). Boxplots on the right-hand side show distributions of the persistence metric across CMIP5 and CMIP6 simulations. The '*' symbol in the column 'ERA/IV' shows the reanalysis estimate and the boxplot is an estimate of the expected agreement given internal variability (see text.) 19 100
- 55 S17 As Fig. S9 but for the AGP index and for the PAC domain (90-270E, 50-75N). Persistence of blocking events (a,b - median, c,d - 90th percentile) for boreal summer. The left-hand side of each panel shows metrics for PRIMAVERA simulations at different grid spacings (resolutions). Boxplots on the right-hand side show distributions of the persistence metric across CMIP5 and CMIP6 simulations. The '*' symbol in the column 'ERA/IV' shows the reanalysis estimate and the boxplot is an estimate of the expected agreement given internal variability (see text.) 20 105

S15	Decomposition of blocking bias into (i) a term due to the bias in the number of events (E), (ii) a term due to the bias in persistence (P), and (iii) a cross term (C). Boxplots show the ensemble spread across the CMIP5, CMIP6, and all coupled PRIMAVERA models, respectively. The AGP index with 5-day persistence is used and results are shown for the ATL and PAC domains, and for boreal winter (DJF) and summer (JJA). The blocking bias is normalised by the reanalysis estimate of blocking frequency.	17
5		
10		

List of Tables

S1	CMIP5 simulations used in this study. The r1i1p1 ensemble member from the historical experiment is used for each simulation.	18
15		
S2	CMIP6 simulations used in this study. All simulations are for the historical experiment during 1950–2014.	18

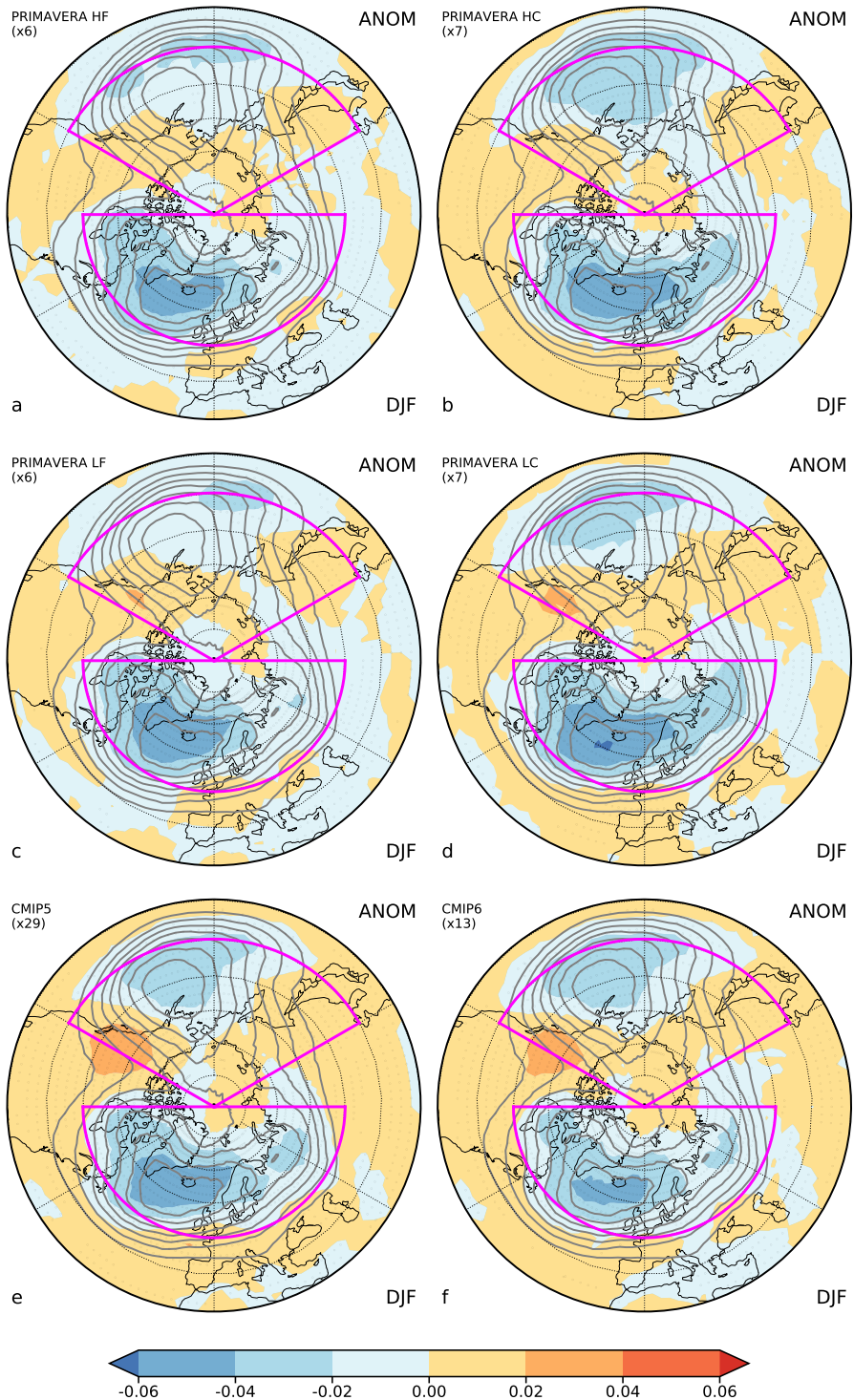


Figure S1. Blocking frequency bias for the ANOM index, boreal winter, and (a) high-resolution forced, (b) high-resolution coupled, (c) low-resolution forced, (d) low-resolution coupled PRIMAVERA simulations, and (e) CMIP5, (f) CMIP6 simulations. Stippling shows agreement on the sign of the bias by at least (a,c) 6 of 6, (b,d) 6 of 7, (e) 19 of 29, and (f) 10 of 13 simulations.

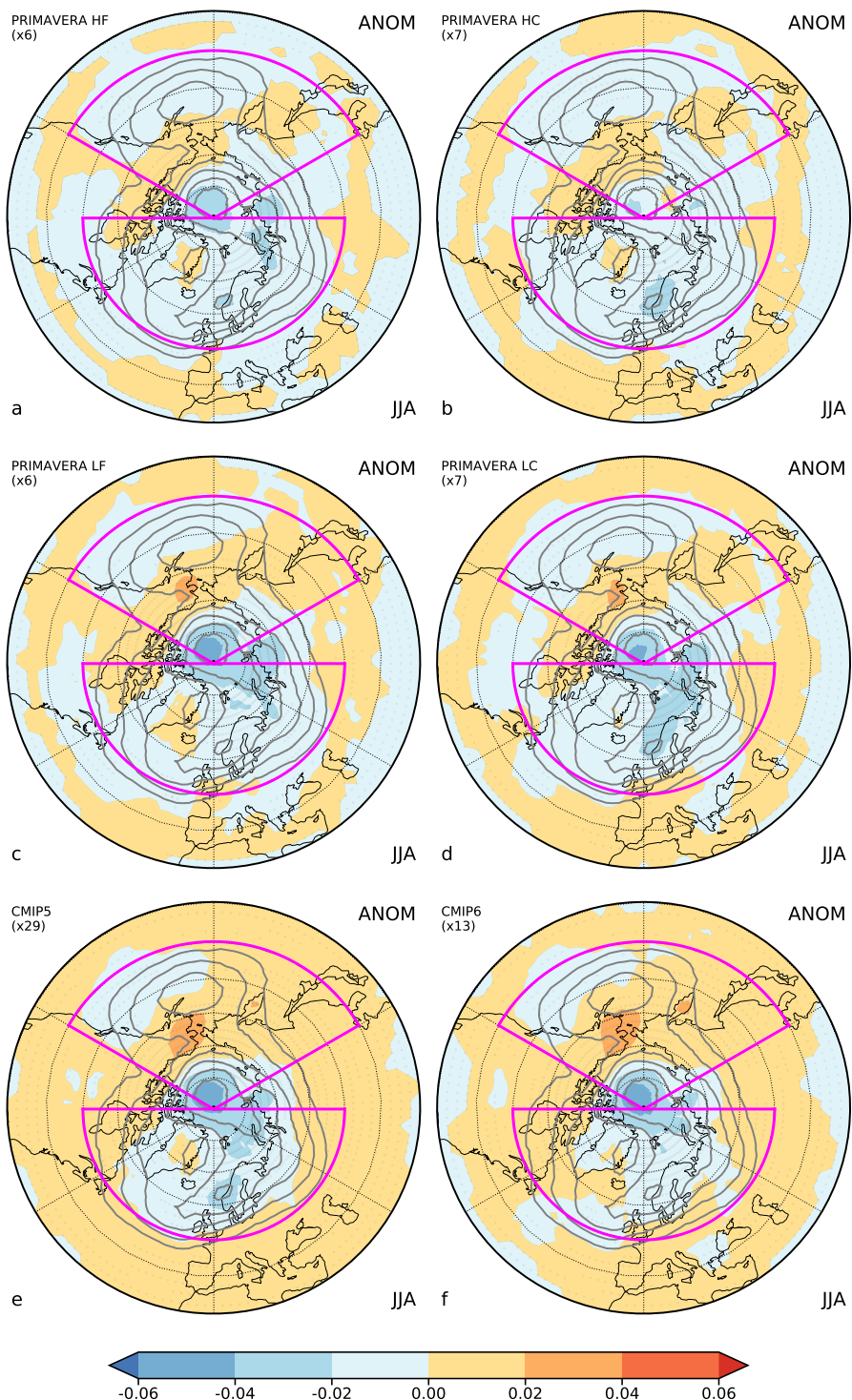


Figure S2. As Fig. S1 but for boreal summer. (Blocking frequency bias for the ANOM index and (a) high-resolution forced, (b) high-resolution coupled, (c) low-resolution forced, (d) low-resolution coupled PRIMAVERA simulations, and (e) CMIP5, (f) CMIP6 simulations. Stippling shows agreement on the sign of the bias by at least (a,c) 6 of 6, (b,d) 6 of 7, (e) 19 of 29, and (f) 10 of 13 simulations.)

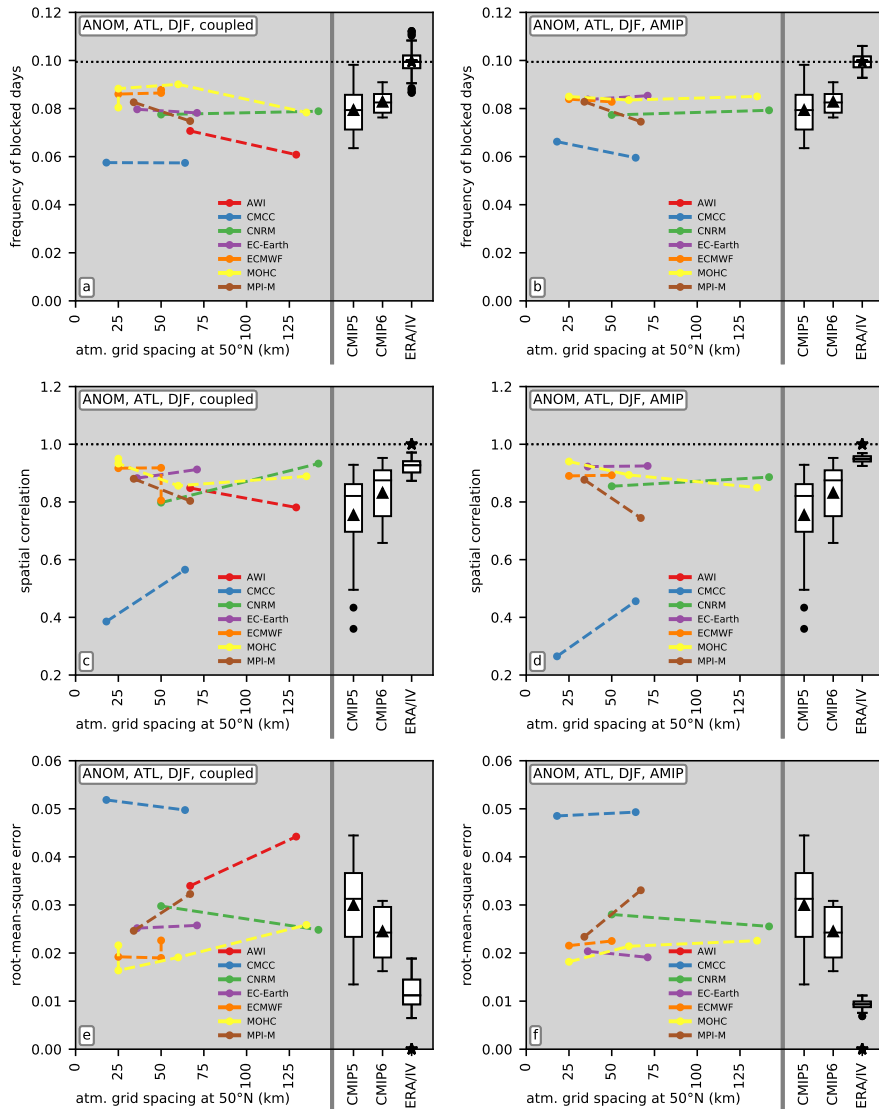


Figure S3. Metrics of blocking performance (a,b - blocking frequency, c,d - spatial correlation, e,f - root-mean-square error) for the ANOM index and boreal winter, for the ATL domain (-90-90E, 50-90N). The left-hand side of each panel shows metrics for PRIMAVERA simulations at different grid spacings (resolutions). Boxplots on the right-hand side show distributions of the metric across CMIP5 and CMIP6 simulations. The '*' symbol in the column 'ERA/IV' shows the reanalysis estimate and the boxplot is an estimate of the expected agreement given internal variability (see text).

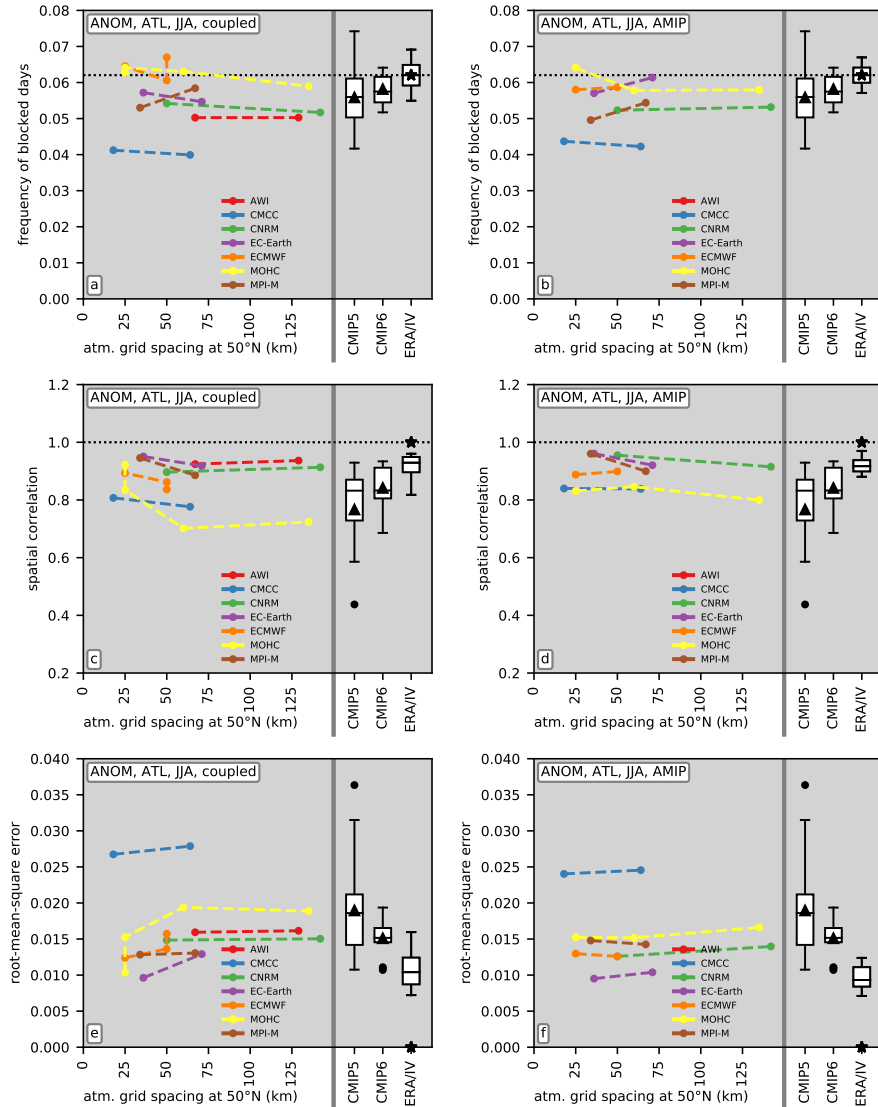


Figure S4. As Fig. S3 but for boreal summer. (Metrics of blocking performance (a,b - blocking frequency, c,d - spatial correlation, e,f - root-mean-square error) for the ANOM index and for the ATL domain (-90-90E, 50-90N). The left-hand side of each panel shows metrics for PRIMAVERA simulations at different grid spacings (resolutions). Boxplots on the right-hand side show distributions of the metric across CMIP5 and CMIP6 simulations. The '*' symbol in the column 'ERA/IV' shows the reanalysis estimate and the boxplot is an estimate of the expected agreement given internal variability (see text).)

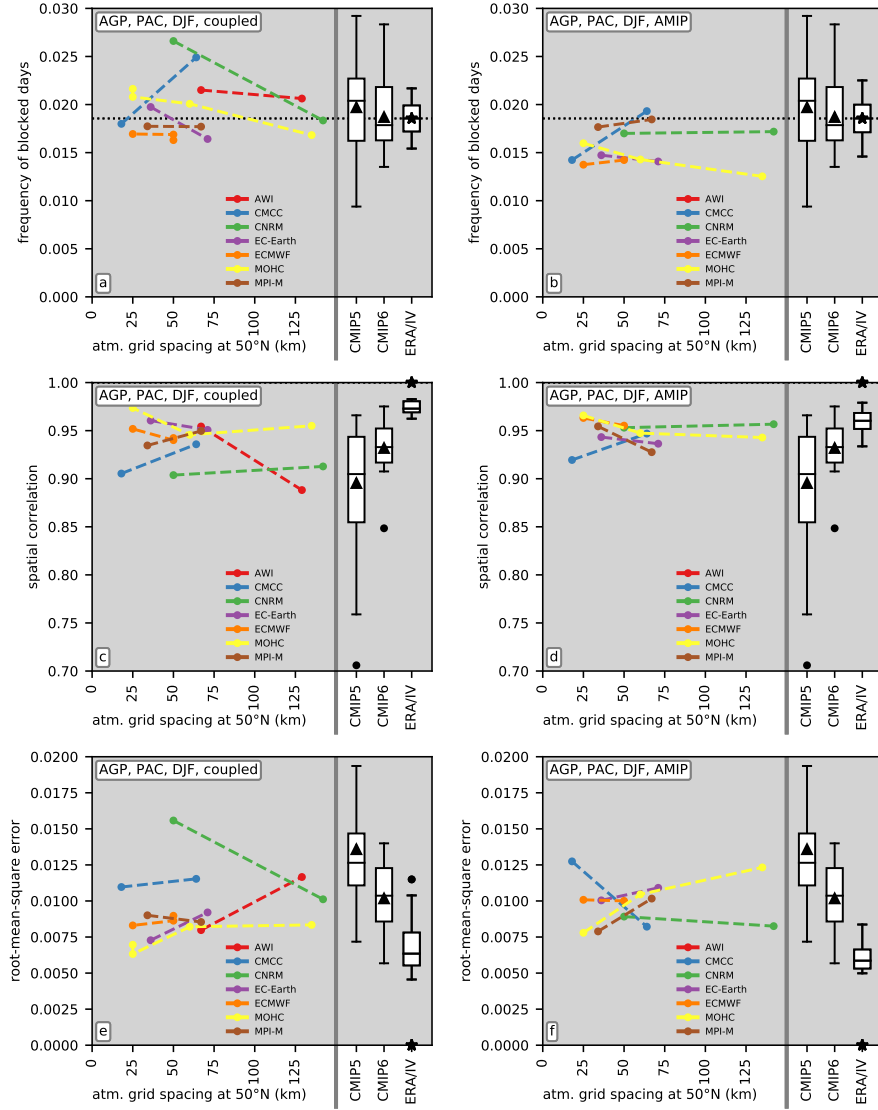


Figure S5. As Fig. S3 but for the AGP index and the PAC domain (90–270E, 50–75N). (Metrics of blocking performance (a,b - blocking frequency, c,d - spatial correlation, e,f - root-mean-square error) for boreal winter. The left-hand side of each panel shows metrics for PRIMAVERA simulations at different grid spacings (resolutions). Boxplots on the right-hand side show distributions of the metric across CMIP5 and CMIP6 simulations. The '*' symbol in the column 'ERA/IV' shows the reanalysis estimate and the boxplot is an estimate of the expected agreement given internal variability (see text).)

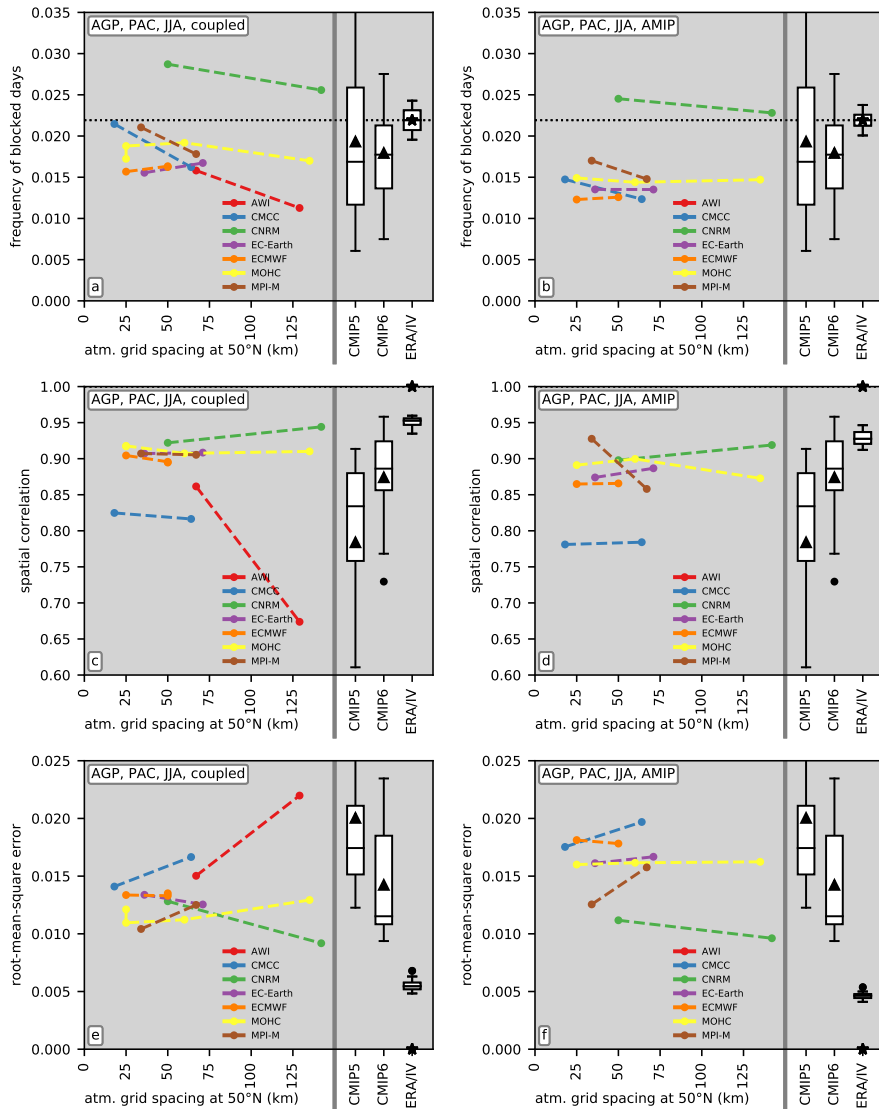


Figure S6. As Fig. S3 but for the AGP index, the PAC domain (90-270E, 50-75N) and boreal summer. (Metrics of blocking performance (a,b - blocking frequency, c,d - spatial correlation, e,f - root-mean-square error). The left-hand side of each panel shows metrics for PRIMAVERA simulations at different grid spacings (resolutions). Boxplots on the right-hand side show distributions of the metric across CMIP5 and CMIP6 simulations. The '*' symbol in the column 'ERA/IV' shows the reanalysis estimate and the boxplot is an estimate of the expected agreement given internal variability (see text).)

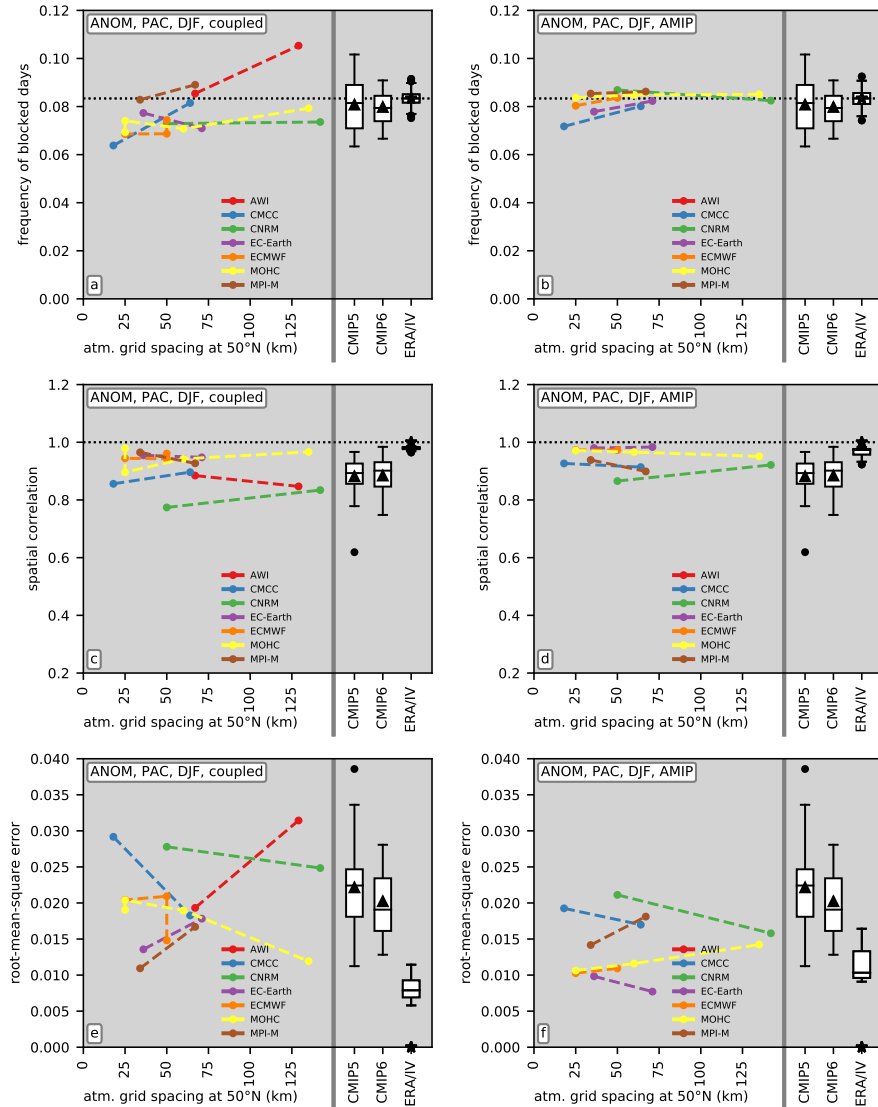


Figure S7. As Fig. S3 but for the PAC domain (120-240E, 40-90N). (Metrics of blocking performance (a,b - blocking frequency, c,d - spatial correlation, e,f - root-mean-square error) for the ANOM index and boreal winter. The left-hand side of each panel shows metrics for PRIMAVERA simulations at different grid spacings (resolutions). Boxplots on the right-hand side show distributions of the metric across CMIP5 and CMIP6 simulations. The '*' symbol in the column 'ERA/IV' shows the reanalysis estimate and the boxplot is an estimate of the expected agreement given internal variability (see text).)

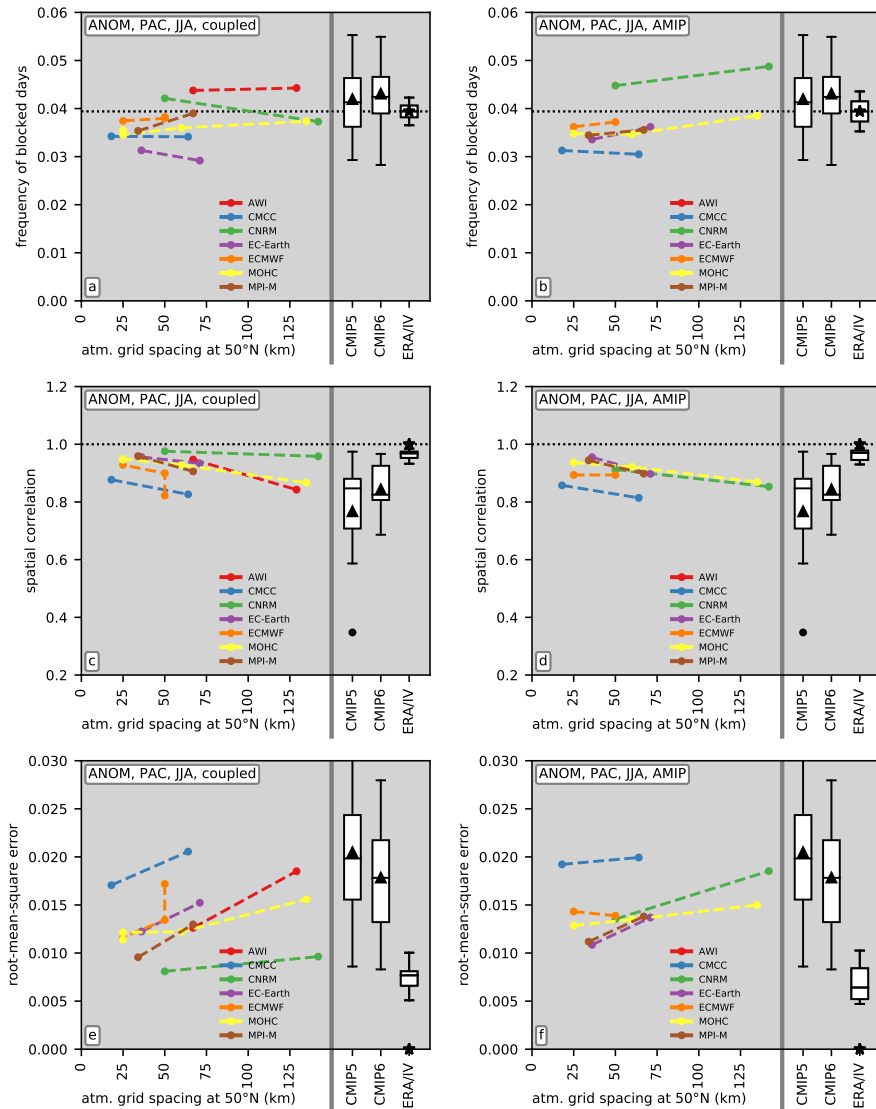


Figure S8. As Fig. S3 but for the PAC domain (120-240E, 40-90N) and boreal summer. (Metrics of blocking performance (a,b - blocking frequency, c,d - spatial correlation, e,f - root-mean-square error) for the ANOM index. The left-hand side of each panel shows metrics for PRIMAVERA simulations at different grid spacings (resolutions). Boxplots on the right-hand side show distributions of the metric across CMIP5 and CMIP6 simulations. The '*' symbol in the column 'ERA/IV' shows the reanalysis estimate and the boxplot is an estimate of the expected agreement given internal variability (see text).)

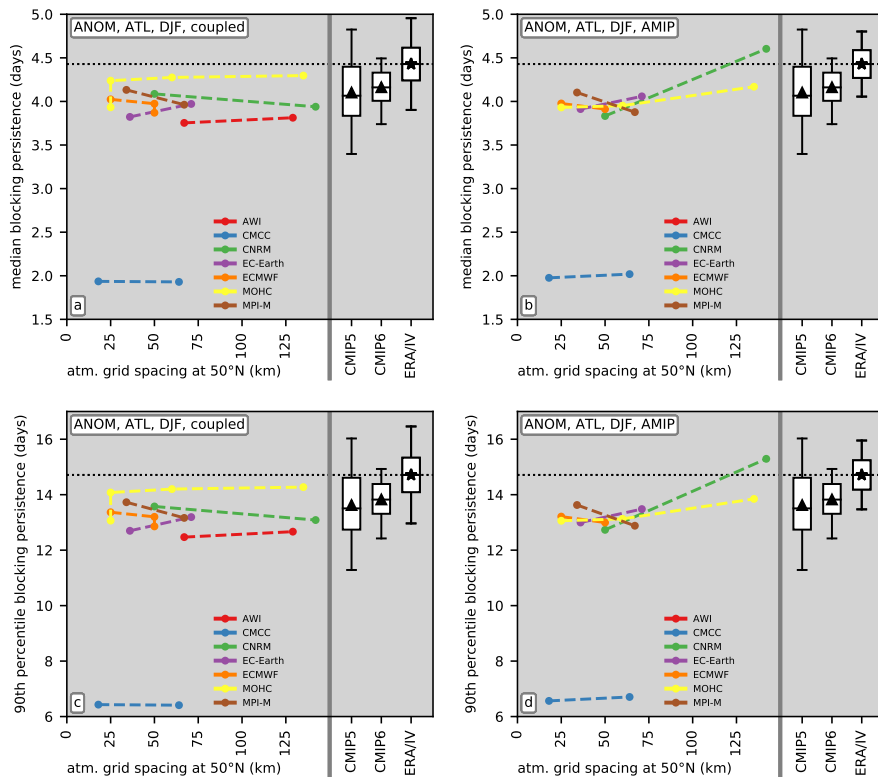


Figure S9. Persistence of blocking events (a,b - median, c,d - 90th percentile) for the ANOM index and boreal winter, for the ATL domain ($-90\text{--}90^\circ\text{E}$, $50\text{--}90^\circ\text{N}$). The left-hand side of each panel shows metrics for PRIMAVERA simulations at different grid spacings (resolutions). The right-hand side shows distributions of the persistence metric across CMIP5 and CMIP6 simulations. The '*' symbol in the column 'ERA/IV' indicates the reanalysis estimate, and the boxplot is an estimate of the expected agreement given internal variability (see text).

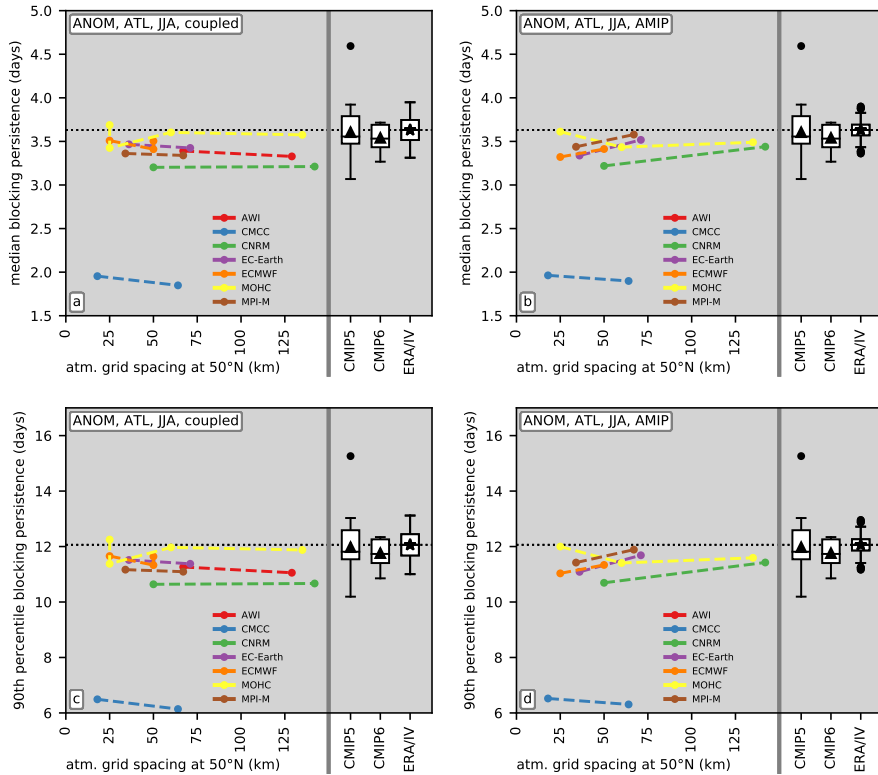


Figure S10. As Fig. S9 but for boreal summer. (Persistence of blocking events (a,b - median, c,d - 90th percentile) for the ANOM index and for the ATL domain (-90-90E, 50-90N). The left-hand side of each panel shows metrics for PRIMAVERA simulations at different grid spacings (resolutions). Boxplots on the right-hand side show distributions of the persistence metric across CMIP5 and CMIP6 simulations. The '*' symbol in the column 'ERA/IV' shows the reanalysis estimate and the boxplot is an estimate of the expected agreement given internal variability (see text).)

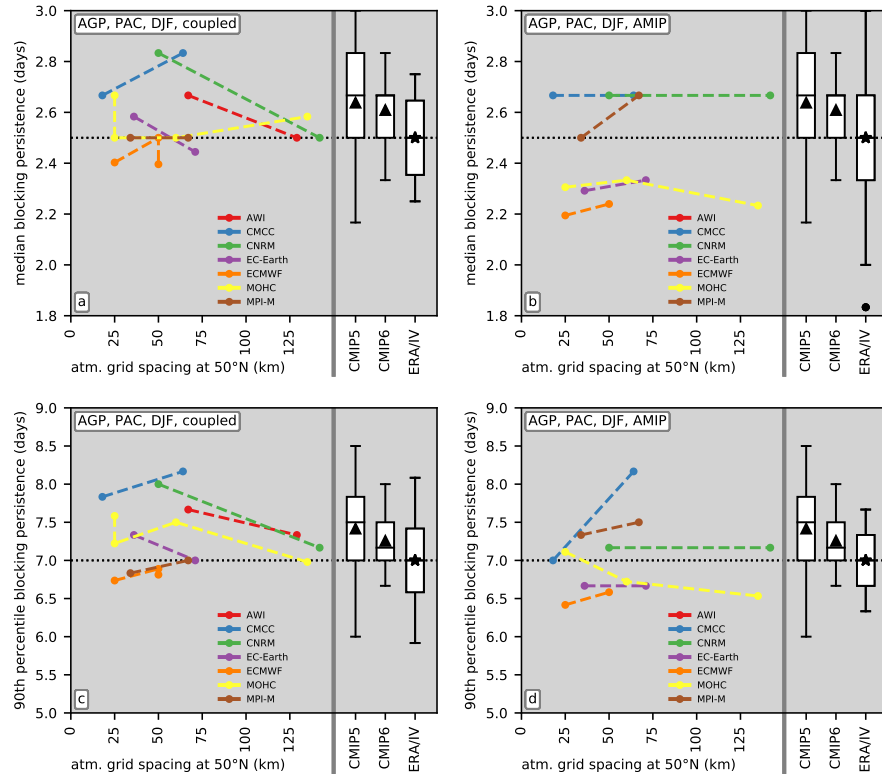


Figure S11. As Fig. S9 but for the AGP index and for the PAC domain (90–270E, 50–75N). Persistence of blocking events (a,b - median, c,d - 90th percentile) for boreal winter. The left-hand side of each panel shows metrics for PRIMAVERA simulations at different grid spacings (resolutions). Boxplots on the right-hand side show distributions of the persistence metric across CMIP5 and CMIP6 simulations. The '*' symbol in the column 'ERA/IV' shows the reanalysis estimate and the boxplot is an estimate of the expected agreement given internal variability (see text).)

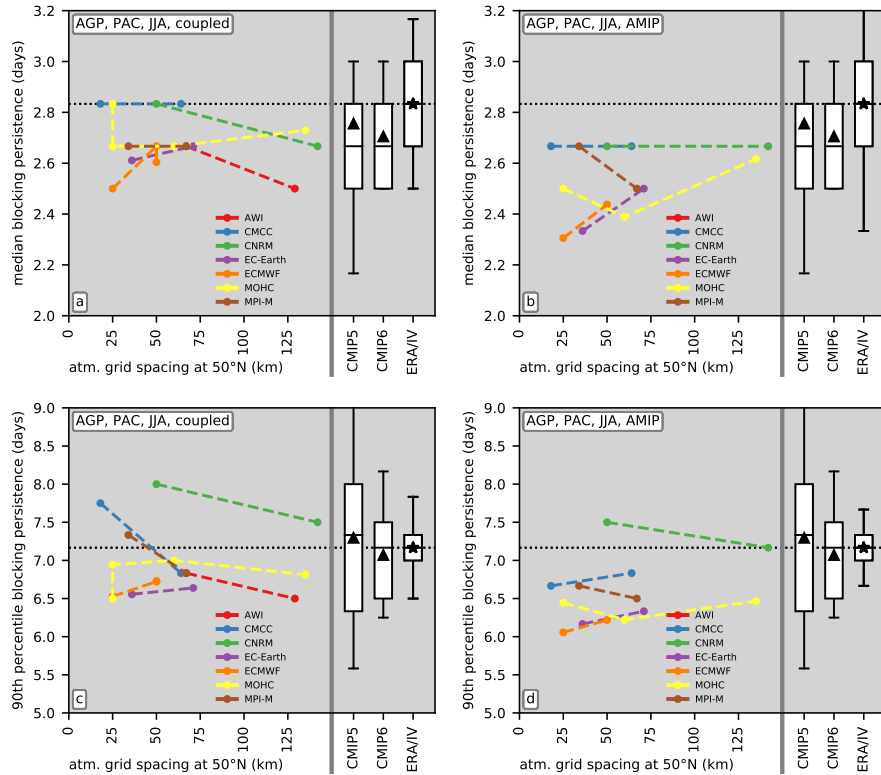


Figure S12. As Fig. S9 but for the AGP index, for the PAC domain (90-270E, 50-75N), and for boreal summer. (Persistence of blocking events (a,b - median, c,d - 90th percentile). The left-hand side of each panel shows metrics for PRIMAVERA simulations at different grid spacings (resolutions). Boxplots on the right-hand side show distributions of the persistence metric across CMIP5 and CMIP6 simulations. The '*' symbol in the column 'ERA/IV' shows the reanalysis estimate and the boxplot is an estimate of the expected agreement given internal variability (see text).)

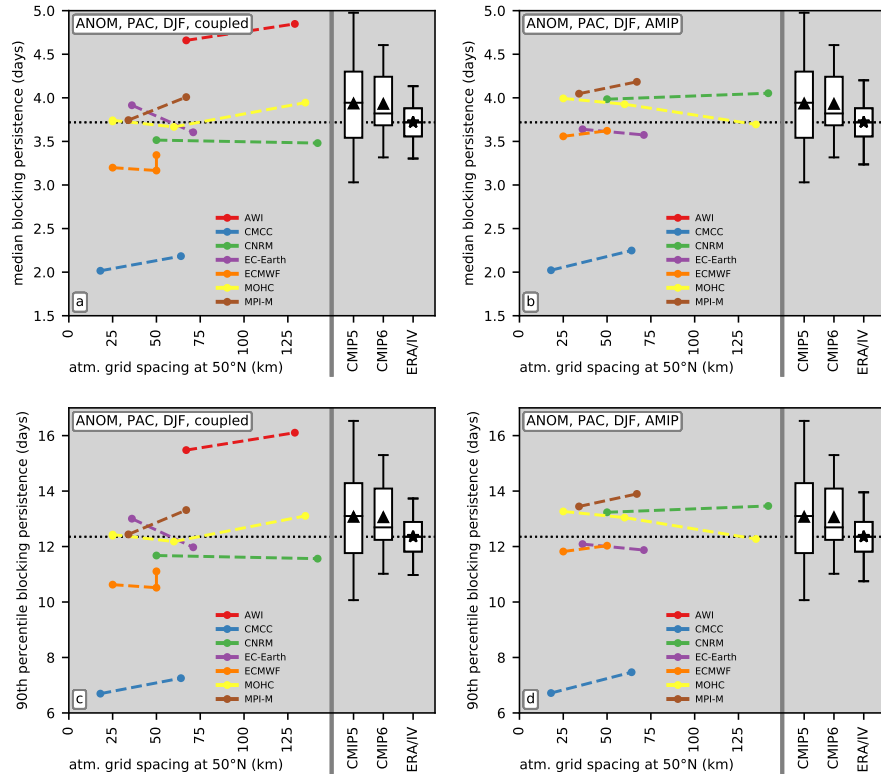


Figure S13. As Fig. S9 but for the PAC domain (120-240E, 40-90N). (Persistence of blocking events (a,b - median, c,d - 90th percentile) for the ANOM index and boreal winter. The left-hand side of each panel shows metrics for PRIMAVERA simulations at different grid spacings (resolutions). Boxplots on the right-hand side show distributions of the persistence metric across CMIP5 and CMIP6 simulations. The '*' symbol in the column 'ERA/IV' shows the reanalysis estimate and the boxplot is an estimate of the expected agreement given internal variability (see text).)

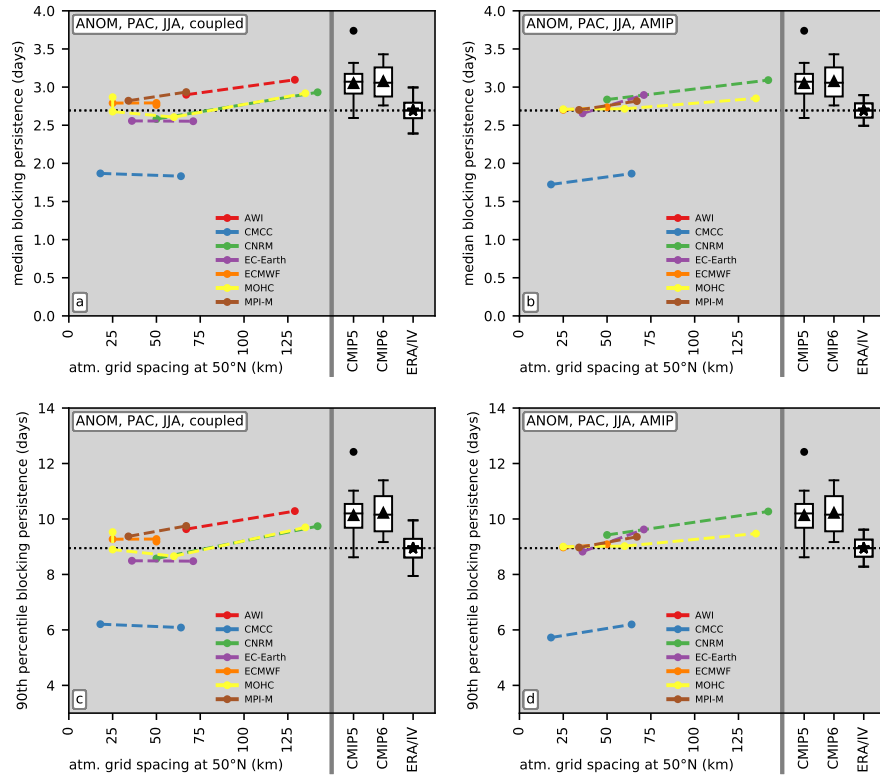


Figure S14. As Fig. S9 but for the PAC domain (120-240E, 40-90N) and boreal summer. (Persistence of blocking events (a,b - median, c,d - 90th percentile) for the ANOM index. The left-hand side of each panel shows metrics for PRIMAVERA simulations at different grid spacings (resolutions). Boxplots on the right-hand side show distributions of the persistence metric across CMIP5 and CMIP6 simulations. The '*' symbol in the column 'ERA/IV' shows the reanalysis estimate and the boxplot is an estimate of the expected agreement given internal variability (see text).)

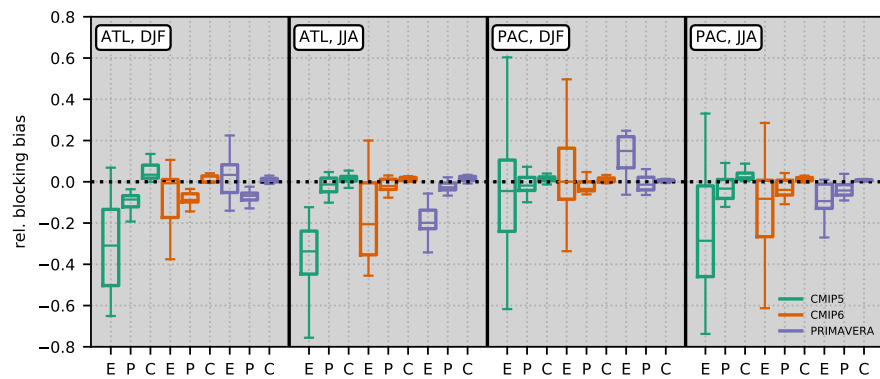


Figure S15. Decomposition of blocking bias into (i) a term due to the bias in the number of events (E), (ii) a term due to the bias in persistence (P), and (iii) a cross term (C). Boxplots show the ensemble spread across the CMIP5, CMIP6, and all coupled PRIMAVERA models, respectively. The AGP index with 5-day persistence is used and results are shown for the ATL and PAC domains, and for boreal winter (DJF) and summer (JJA). The blocking bias is normalised by the reanalysis estimate of blocking frequency.

Table S1. CMIP5 simulations used in this study. The r1i1p1 ensemble member from the historical experiment is used for each simulation.

No.	Centre	Model	Period
1	CSIRO-BOM	ACCESS1-0	1950–2005
2	CSIRO-BOM	ACCESS1-3	1950–2005
3	BCC	BCC-CSM1-1	1950–1997
4	BCC	BCC-CSM1-1-M	1950–2005
5	BNU	BNU-ESM	1950–2005
6	CCCma	CanESM2	1950–2005
7	CMCC	CMCC-CESM	1950–2005
8	CMCC	CMCC-CM	1950–2005
9	CMCC	CMCC-CMS	1950–2005
10	CNRM-CERFACS	CNRM-CM5	1950–2005
11	EC-Earth-Consortium	EC-EARTH	1950–2005
12	LASG-CESS	FGOALS-g2	1950–2005
13	NOAA-GFDL	GFDL-CM3	1950–2005
14	NOAA-GFDL	GFDL-ESM2G	1950–2005
15	MOHC	HadCM3	1960–2005
16	MOHC	HadGEM2-CC	1950–2005
17	MOHC	HadGEM2-ES	1981–2005
18	IPSL	IPSL-CM5A-LR	1950–2005
19	IPSL	IPSL-CM5A-MR	1950–2005
20	IPSL	IPSL-CM5B-LR	1950–2005
21	MIROC	MIROC5	1950–2005
22	MIROC	MIROC-ESM-CHEM	1950–2005
23	MIROC	MIROC-ESM	1950–2005
24	MPI-M	MPI-ESM-LR	1950–2005
25	MPI-M	MPI-ESM-MR	1950–2005
26	MPI-M	MPI-ESM-P	1950–2005
27	MRI	MRI-CGCM3	1950–2005
28	MRI	MRI-ESM1	1950–2005
29	NCC	NorESM1-M	1950–2005

Table S2. CMIP6 simulations used in this study. All simulations are for the historical experiment during 1950–2014.

No.	Centre	Model	Ensemble member
1	BCC	BCC-CMS2-MR	r1i1p1f1
2	BCC	BCC-ESM1	r1i1p1f1
3	CCCma	CanESM5	r1i1p1f1
4	CNRM-CERFACS	CNRM-CM6-1	r2i1p1f2
5	CNRM-CERFACS	CNRM-ESM2-1	r3i1p1f2
6	IPSL	IPSL-CM6A-LR	r1i1p1f1
7	MOHC	HadGEM3-GC31-LL	r1i1p1f3
8	MOHC	UKESM1-0-LL	r1i1p1f2
9	MRI	MRI-ESM2-0	r1i1p1f1
10	NASA-GISS	GISS-E2-1-G	r1i1p1f1
11	NCAR	CESM2	r1i1p1f1
12	NCAR	CESM2-WACCM	r2i1p1f1
13	NOAA-GFDL	GFDL-CM4	r1i1p1f1